Release-Dependent Variations in Synaptic Latency: A Putative Code for Short- and Long-Term Synaptic Dynamics

Sami Boudkkazi,[1,2] Edmond Carlier,[1,2] Norbert Ankri,[1,2] Olivier Caillard,[1,2] Pierre Giraud,[1,2] Laure Fronzaroli-Molinieres,[1,2] and Dominique Debanne[1,2,*]
[1]INSERM U641, Marseille, F-13916 France
[2]Université de la Méditerranée, Faculté de Médecine secteur nord, IFR 11, Marseille, F-13916 France
*Correspondence: dominique.debanne@univmed.fr
DOI 10.1016/j.neuron.2007.10.037

SUMMARY

In the cortex, synaptic latencies display small variations ($\sim$1-2 ms) that are generally considered to be negligible. We show here that the synaptic latency at monosynaptically connected pairs of L5 and CA3 pyramidal neurons is determined by the presynaptic release probability (Pr): synaptic latency being inversely correlated with the amplitude of the postsynaptic current and sensitive to manipulations of Pr. Changes in synaptic latency were also observed when Pr was physiologically regulated in short- and long-term synaptic plasticity. Paired-pulse depression and facilitation were respectively associated with increased and decreased synaptic latencies. Similarly, latencies were prolonged following induction of presynaptic LTD and reduced after LTP induction. We show using the dynamic-clamp technique that the observed covariation in latency and synaptic strength is a synergistic combination that significantly affects postsynaptic spiking. In conclusion, amplitude-related variation in latency represents a putative code for short- and long-term synaptic dynamics in cortical networks.

INTRODUCTION

Nerve cells transmit information not only by their firing rate but also by the temporal organization of their discharge (Rieke et al., 1997). Temporally organized spiking in cortical networks is crucial for coding sensory information (Singer 1999), induction of synaptic plasticity (Debanne et al., 1998; Bi and Poo, 1998) and synchronization of network activity (König et al., 1996). In simple neuronal circuits, the timing of neuronal activity is determined by the interplay between geometrical factors and synaptic and voltage-gated currents. At the postsynaptic side, timing of spike generation is controlled by intrinsic and synaptic mechanisms (Fricker and Miles, 2000; Pouille and Scan-

ziani, 2001; Sourdet et al., 2003). The timing between connected neurons is usually described by the synaptic latency, which is the sum of the axonal conduction time, determined by the axonal length and the conduction velocity, and the synaptic delay (Sabatini and Regher, 1999). Synaptic latencies in the cortex range between 0.2 and 6 ms (Markram et al., 1997; Feldmeyer et al., 1999), and this large variability is thought to enrich the storage capacity of neural networks (Izhikevitch, 2006). Axonal conduction is temporally very precise but can be affected by the presence of branch points and swellings on the axon and by local voltage-gated currents (review in Debanne, 2004). The synaptic delay is the consequence of a cascade of molecular events linking the depolarization of the presynaptic terminal by the sodium spike to the release of neurotransmitter (review in Meinrenken et al., 2003). In giant synapses, synaptic delay is largely determined by presynaptic Ca^{2+} influx (Bollmann et al., 2000; Schneggenburger and Neher, 2000; Feldchyshyn and Wang, 2007) and the waveform of the presynaptic AP (Katz and Miledi, 1967; Augustine et al., 1985), but how synaptic timing is controlled at cortical synapses has yet to be determined.

In cortical circuits, the synaptic latency at monosynaptic connections varies within $\sim$1–2 ms (Miles and Wong, 1986; Debanne et al., 1995; Markram et al., 1997). These small variations are generally considered to be functionally negligible, and therefore synaptic latency is often considered to be a constant parameter. We show here that latency at connected pairs of L5 cortical pyramidal neurons is not fixed but rather is determined by the presynaptic release probability (Pr). Our data provide evidence for a direct relationship between synaptic strength and synaptic timing in physiological conditions. This release-dependent process constitutes a putative temporal code for the efficacy of cortical synaptic strength.

RESULTS

Dependence of Synaptic Latency on Quantal Content

Monosynaptic connections were observed in 151 of 426 pairs of adjacent L5 pyramidal neurons (probability of
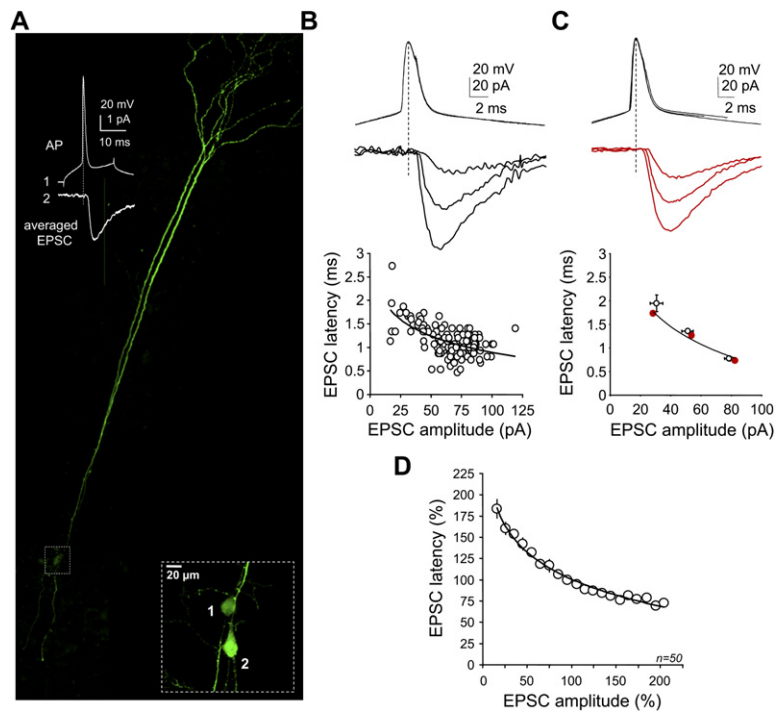
Figure 1. Amplitude-Dependent Latency Variation at L5-L5 Synapse

(A) Confocal reconstruction of a connected pair of L5 pyramidal neurons labeled with biocytin. (Top left) Synaptic coupling: an AP evoked in neuron 1 elicited an EPSC in neuron 2. (Bottom right) High magnification of the cell bodies.

(B) Amplitude-dependent latency variations at the synapse formed by two L5 neurons. (Upper traces) Representative presynaptic APs (1) and evoked postsynaptic currents (2). (Lower graph) EPSC latency versus EPSC amplitude ($y = -0.5Ln(x) + 3.2$; $R^2 = 0.35$).

(C) Same connection. (Upper traces) Individual EPSCs were sorted according to their amplitude in three groups and averaged (n = 6 trials). (Lower graph) EPSC latency versus EPSC amplitude for averaged EPSCs (red ●) and for the mean of individual EPSCs in these averages (○). Note the nonlinear inverse correlation ($y = -0.9Ln(x) + 4.8$; $R^2 = 0.98$). Error bars show SEM.

(D) Normalized pooled data over 50 L5-L5 synapses ($y = -46Ln(x) + 313$, $R^2 = 0.98$).

35%). The analysis was restricted to 50 connections with a mean amplitude larger than 10 pA. The latency of individual EPSCs was measured from the peak of the presynaptic AP measured in the cell body to 5% of the EPSC amplitude (Figure S1 available online). The mean EPSC latency was near 1 ms (1.21 ± 0.07 ms; n = 50; range: 0.2/4 ms), but this value is underestimated when the reference is the presynaptic AP measured in the cell body. Simultaneous somatic and axonal recordings showed that the conduction time from the site of initiation in the axon (5–60 μm) to the soma was ∼0.4 ms (Figure S2). In individual L5-L5 pairs (Figure 1A), EPSC latency was found to fluctuate from trial to trial in a stationary way, whereas synaptic latency was inversely related to EPSC amplitude. Large EPSCs had a short latency, whereas small EPSCs had a longer latency (Figure 1B). The variation in latency was in the millisecond range. To eliminate the potential impact of recording noise, individual EPSCs were averaged according to their amplitudes into three main groups. In the same connection, the latency of small averaged EPSCs was clearly longer than that of large averaged EPSCs (Figure 1C). A similar inverse correlation was observed across the whole set of connections (Figure 1D).

In these experiments, the presynaptic spike jitter was not considered. However, presynaptic spike latency may fluctuate from trial to trial, thus eventually blurring the latency versus amplitude relation. To test this hypothesis, L5 pyramidal neurons were recorded in cell-attached configuration, and postsynaptic APs were triggered by EPSPs evoked by stimulating layer II/III. The stimulus intensity was adjusted to produce a spike in 50% of cases (Figure 2A). The standard deviation of the spike latency

evoked in these conditions was 0.58 ± 0.05 ms (Figure 2B), confirming previous observations in the hippocampus (Pouille and Scanziani, 2001). Next, the relation between this presynaptic jitter and the latency versus amplitude correlation was evaluated in six pairs. Although the introduction of a jitter of 0.58 ms by convolution of a random Gaussian distribution with the latency population decreased the coefficient of correlation (Figure 2C), among 10^5 random draws (see Experimental Procedures), the probability of observing a significant inverse correlation between latency and amplitude ($p < 0.05$ or $p < 0.005$) remained very high (96% ± 2%, n = 6 for $p < 0.05$ and 84% ± 7%, n = 6 for $p < 0.005$, Figure 2D).

Presynaptic Origin of Amplitude-Dependent Variation in Latency

The differential timing of small and large EPSCs could be due to the fact that these synaptic responses result from activation of synapses located at different dendritic regions. The most distal synapses would produce responses attenuated by postsynaptic dendritic filtering. In this case, small EPSCs should have slower kinetics, hence longer latencies. However, no significant difference in the time-to-peak could be detected between maximal (100%) and small EPSCs (10%–90% of the maximal EPSC amplitude; 91% ± 2%, n = 50, Mann-Whitney $p > 0.1$, Figure 3A). Thus, the observed difference in latency between large and small EPSCs cannot be explained by differential dendritic filtering on the postsynaptic side.

Alternatively, the long latencies measured for small EPSCs could correspond to an error in latency measurement because the signal-to-noise ratio is lower for small
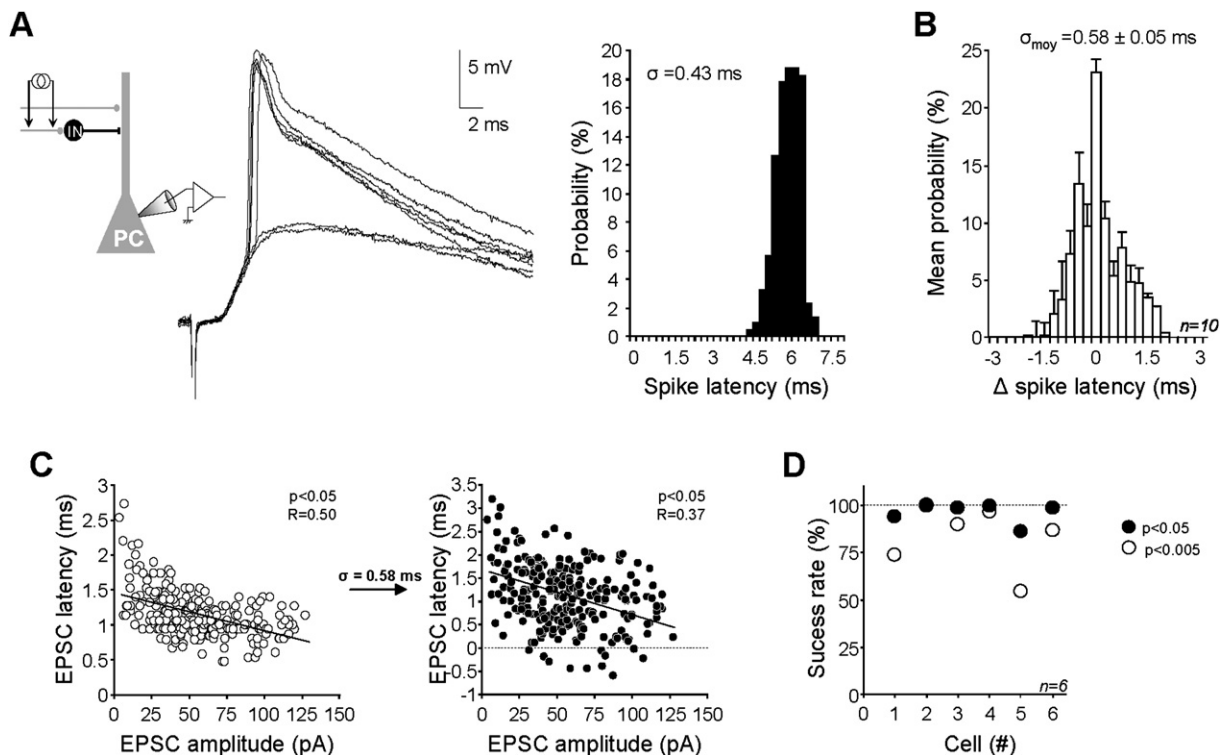
Figure 2. The Jitter of the Presynaptic Spike Does Not Suppress *Pr*-Dependent Latency Correlation in L5 Pyramidal Cells

(A) Evaluation of the jitter in L5 pyramidal neurons. (Left) Experimental configuration. L5 neurons were recorded in cell-attached configuration, and a compound synaptic pathway was evoked by stimulating the layer II/III. A postsynaptic spike was evoked by the compound EPSP in ∼50% of the cases. (Right) Histogram of spike latency (jitter, σ = 0.43 ms; bin size = 0.25 ms).
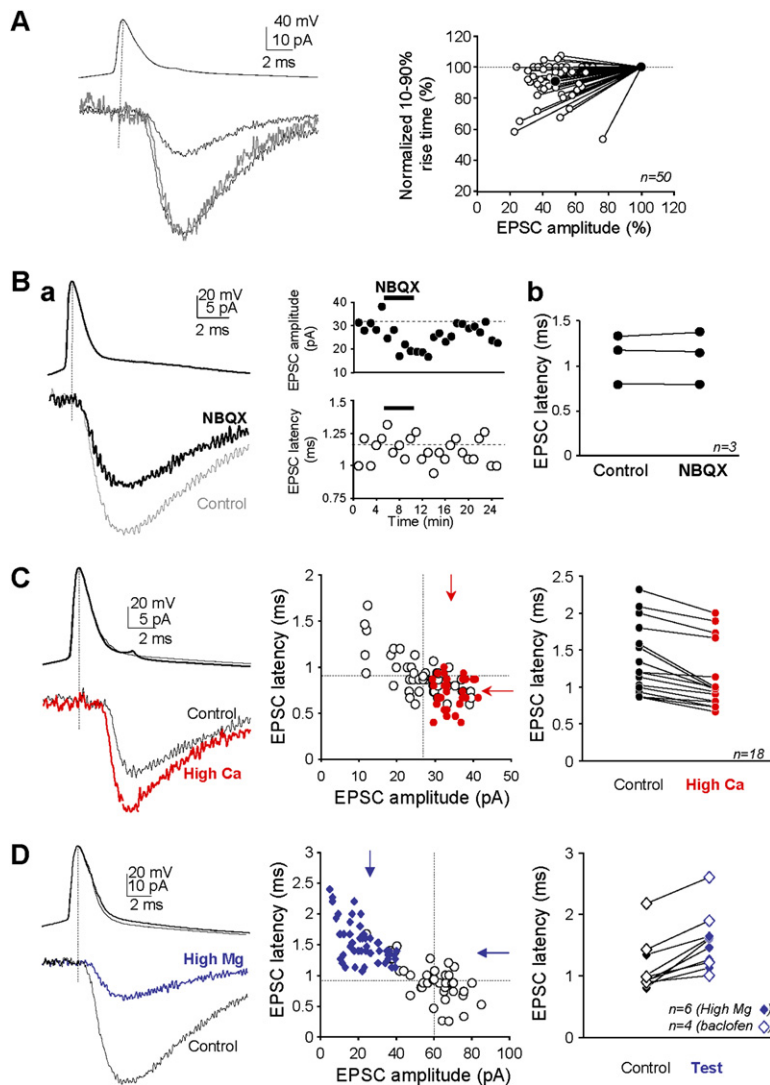
(B) Pooled variations in spike latency over ten neurons (aligned on the mode). Error bars show SEM.

(C) To test the effect of the jitter on the amplitude-dependent latency variation, a Gaussian jitter of 0.58 ms was convolved with the latency distribution. (Left) Data from a single L5-L5 pair. Exceptionally, the data were linearly fitted to facilitate the analysis. (Right) Distribution after convolution with a Gaussian jitter of 0.58 ms. Note the increase in the dispersion of the data points but the robustness of the correlation.

(D) Success rate for six neurons as in (C). The success rate expresses the rate of random drawings, providing a significant correlation with a criterion at p < 0.05 or p < 0.005.

signals. To test this hypothesis, the amplitude of EPSCs was reduced to half of the control (48% ± 14%, n = 3) by partial blockade of postsynaptic AMPA receptors with 0.4 μM NBQX. Synaptic latency was, however, not significantly affected (from 1.10 ± 0.16 to 1.12 ± 0.17 ms, n = 3; paired t test p > 0.1; Figure 3B), indicating that the measurement of long latencies for small EPSCs is not due to poor signal detection. Furthermore, when the impact of noise on the synaptic latency was estimated with EPSCs simulated with Igor Pro (WaveMetrics), the latencies in our experiments were not significantly affected when the signal-to-noise ratio was greater than 3 (a condition always respected in our experiments). In fact, even large Gaussian noise of 10 pA had virtually no effect on the latency of EPSCs greater than 20/30 pA (Figure S3). We also tested the effect on latency of changing the driving force for AMPA receptor-mediated currents. Moving the holding potential from −70 mV to −50 mV reduced the EPSC amplitude (67% ± 5% of the control amplitude, n = 6) but did not change the latency (1.31 ± 0.22 ms versus 1.31 ± 0.22 ms, n = 6, paired t test, p > 0.5; data not shown).

If postsynaptic filtering and detection of small synaptic responses are not responsible for the dependence we observed, presynaptic glutamate release may underlie the variation in latency. *Pr* was manipulated via modification of the extracellular [Ca^{2+}] to [Mg^{2+}] ratio or by application of the GABA$_B$ receptor agonist baclofen. Increasing the extracellular [Ca^{2+}] to [Mg^{2+}] ratio (from 3 mM Ca^{2+} and 2 mM Mg^{2+} to 5 mM Ca^{2+} and 0.5 mM Mg^{2+}) enhanced synaptic transmission (173% ± 14% of the control EPSC amplitude, n = 18) and decreased synaptic latency (83% ± 2% of the control latency, n = 18, Figure 3C; from 1.32 ± 0.10 to 1.09 ± 0.09 ms, n = 18, paired t test p < 0.05). Conversely, when this ratio was decreased (from 3 mM Ca^{2+} and 2 mM Mg^{2+} to 1 mM Ca^{2+} and 3 mM Mg^{2+}) synaptic transmission was reduced (35% ± 8% of the control EPSC amplitude, n = 6), and synaptic latency was increased by about 0.5 ms (from 0.99 ± 0.08 to 1.45 ± 0.09 ms, n = 6, paired t test p < 0.01; 145% ± 14% of the control, Figure 3D). Similar effects were also observed on multiunitary postsynaptic potentials (EPSPs) elicited by extracellular stimulation (mean latency 2.56 ± 0.16 ms in 1 mM Ca^{2+} and 3 mM Mg^{2+} versus

Figure 3. Pre- but Not Postsynaptic Origin of Amplitude-Dependent Latency at L5-L5 Connections

(A) Comparison of the time course of small and large EPSCs at L5-L5 synapse. (Left) Scaling of small and large EPSCs at a synapse formed by a pair of L5 pyramidal neurons. Each trace corresponds to an average over six trials. Thick gray trace: scaled small EPSC. (Right) Normalized EPSC rise time (10%–90%) against EPSC amplitude. For each synapse, large averaged EPSCs were normalized to 100%. The large black circle corresponds to the mean.

(B) Partial blockade of AMPA receptors with NBQX (0.4 μM) reduced EPSC amplitude without affecting EPSC latency. (Ba) (Left) Synaptic currents evoked in control and in the presence of NBQX. (Right) Time course of the effect of NBQX on EPSC amplitude (top) and latency (bottom). (Bb) Group data corresponding to the three pairs tested.

(C) Effect of increasing Pr on synaptic latency. Increasing the extracellular $[Ca^{2+}]$ to $[Mg^{2+}]$ ratio (from 3 mM Ca^{2+} and 2 mM Mg^{2+} [control] to 5 mM Ca^{2+} and 0.5 mM Mg^{2+} [High Ca]) enhanced synaptic transmission and decreased synaptic latency. (Middle) Plot of EPSC latencies versus amplitudes measured on individual currents in control (○) and in High Ca (red ●). Note the rightward shift of the data and the reduced latency. Mean values of EPSCs and latencies in controls are symbolized by dotted lines and by arrows in High Ca. (Right) Summary of 18 experiments.

(D) Effect of decreasing Pr on synaptic latency. The reduction of the extracellular $[Ca^{2+}]$ to $[Mg^{2+}]$ ratio (from 3 mM Ca^{2+} and 2 mM Mg^{2+} [control] to 1 mM Ca^{2+} and 3 mM Mg^{2+} [High Mg]) or the application of baclofen (◇) decreased synaptic transmission and enhanced synaptic latency. (Middle) Plots of synaptic latency versus EPSC amplitude measured on individual currents in control (○) and in High Mg (◆). Note the leftward shift of the amplitude data and the increased latency (horizontal arrows). (Right) Summary of six and four experiments.

1.67 ± 0.19 ms in 5 mM Ca^{2+} and 0.5 mM Mg^{2+}, n = 8; paired t test, p < 0.05; Figure S4A). In the presence of baclofen (20–60 μM), EPSC amplitude was reduced (to 54% ± 9% of the control amplitude, n = 4), and synaptic latency increased to 124% ± 4% of the control (n = 4; Mann-Whitney, p < 0.01; Figure 3D). Thus, our results show that synaptic latency depends on Pr at connections between L5 pyramidal cells.

EPSPs between L5 neurons are mediated by the release of transmitter from several sites (Markram et al., 1997). One cannot exclude the possibility that release sites have distinct latencies, and the actual latency could be determined by the release site with the shortest latency. Thus, short latencies would be measured when Pr is high, because all sites are recruited, whereas longer latencies would be measured with a low Pr. This hypothesis

predicts that short latencies could occur when Pr is high or low. To test this possibility, the distributions of latency were compared in the same pairs when the $[Ca^{2+}]$ to $[Mg^{2+}]$ ratio varied from 1/3 to 5/0.5. Speaking against this hypothesis, events with short latencies were encountered only in high Ca, not in high Mg (Figure S4B). In fact, the first latency bin was shifted by 0.37 ± 0.09 ms (n = 4). Thus, selective sampling of short latencies within a distribution does not represent a consequential mechanism for Pr-dependent variation in latency.

Latency Variation during Short-Term Synaptic Plasticity

Paired-pulse plasticity at unitary cortical synapses is largely determined by presynaptic mechanisms (Zucker and Regher, 2002). To test whether synaptic latency is
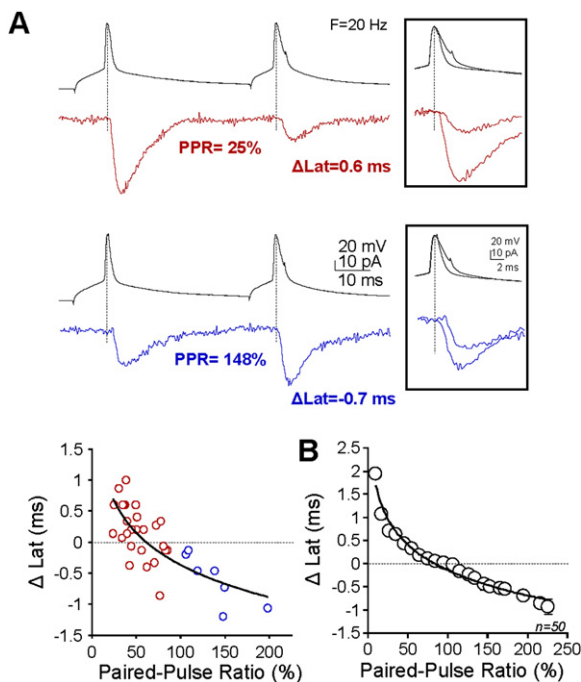
Figure 4. Synaptic Latency during Short-Term Synaptic Plasticity at L5-L5 Connections Tested with Pairs of Presynaptic APs (ISI = 50 ms)

(A) Positive synaptic latency difference (ΔLatency) is associated with PPD (upper traces), whereas negative synaptic ΔLatency is associated with PPF (bottom traces). (Right boxes) Superimposition of currents aligned on the presynaptic APs. (Bottom left) Plot of ΔLatency as a function of the PPR (y = −0.75Ln(x) + 3.09; R^2 = 0.592).

(B) Pooled data over 50 synapses (y = −0.79Ln(x) + 3.50, R^2 = 0.97). Error bars show SEM.

affected by induction of short-term plasticity, pairs of APs were elicited every 10 s in presynaptic L5 pyramidal cells at intervals of 50 ms. Although paired-pulse depression (PPD) dominates at this synaptic connection in young rats (Thomson et al., 1993; Reyes and Sakmann., 1999), the paired-pulse ratio (PPR) varied considerably from trial to trial, and both paired-pulse facilitation (PPF) and PPD were observed at the same connection. The amplitude of the second EPSC (EPSC2) was inversely correlated with the amplitude of the first EPSC (EPSC1) (Figure S5), suggesting that quantal fluctuation determines subsequent release (Debanne et al., 1996). We analyzed the variation in latency (ΔLat = latency$_{EPSC1}$ − latency$_{EPSC2}$) as a function of PPR. PPD was associated with a relative increase in synaptic latency of EPSC2 (positive ΔLat), whereas PPF was associated with a relative decrease in latency (negative ΔLat). In fact, the variation in latency was cumulative during short-term plasticity (range of ± 1 ms) and was negatively correlated with the PPR (Figure 4A). To eliminate the potential impact of recording noise, individual traces were averaged according to their PPR into two main groups (one group with PPD and the other with PPF). Consistent with the previous observation, the variation in

latency measured on averaged traces clearly depended upon PPR. This dependency was observed in all studied connections (n = 50, Figure 4B) when the postsynaptic cell was recorded in current-clamp (Figure S6), thus confirming that latency varies as a function of PPR.

To provide further evidence that latency is influenced by short-term synaptic plasticity, we changed PPR by modifying the extracellular [Ca^{2+}] to [Mg^{2+}] ratio. In saline containing a high [Ca^{2+}]/[Mg^{2+}] ratio, PPR decreased (from 62% ± 4% to 38% ± 4%, n = 8, paired t test p < 0.01), and the proportion of positive ΔLat increased (from 69% ± 4% to 77% ± 4% n = 8, paired t test p < 0.01; Figures S7A and S7B). Conversely, in saline containing a low [Ca^{2+}]/[Mg^{2+}] ratio, PPR increased (from 56% ± 3% to 122% ± 10%, n = 6, paired t test p < 0.01), and the proportion of positive ΔLat decreased (from 63% ± 5% to 35% ± 6%, n = 6, paired t test p < 0.01; Figures S7C and S7D). Therefore, variations in latency are observed during short-term plasticity and depend upon the PPR.

During paired-pulse stimulation, the second presynaptic spike was generally broader than the first one, which may affect synaptic latency (reviewed in Lin and Faber, 2002). We therefore investigated whether spike broadening was also present in the axon or only in the soma. Simultaneous whole-cell recordings from the cell body and "loose-patch" recordings from the proximal part of the axon (10–170 μm) were obtained from L5 pyramidal neurons. Pairs of APs were evoked with an interval of 50 ms. Half-width of the second AP increased in the cell body (1.49 ± 0.06 ms versus 1.67 ± 0.07 ms for the second AP, n = 10), but the AP waveform recorded in the axon remained unchanged during the second stimulation (Figure S8). Thus, the changes in latency observed during paired-pulse plasticity are not a consequence of a modification of the presynaptic spike width but may rather correspond to a mechanism involving the presynaptic release machinery.

Release-Dependent Variation in Latency Is a General Principle

Release-dependent variation in latency is present at L5-L5 connections, but it is not clear whether it is a general feature of central synapses. To address this question, we examined whether facilitating synapses also display release-dependent variations in latency. Pairs of CA3 pyramidal neurons were recorded in hippocampal slice cultures (Gähwiler, 1981; Debanne et al., 1995). Twelve out of thirty pairs were connected, and in six connections, the amplitude of the mean evoked EPSC was larger than 15 pA. Release- and PPR-dependent variations in latency were observed at CA3-CA3 synaptic connections (Figure S9), suggesting that amplitude dependence of latency is a general principle at central synapses.

Latency Variations Resulting from Long-Term Synaptic Plasticity

Long-term synaptic plasticity at L5 pyramidal cell connections is associated with a change in the PPR (Markram and
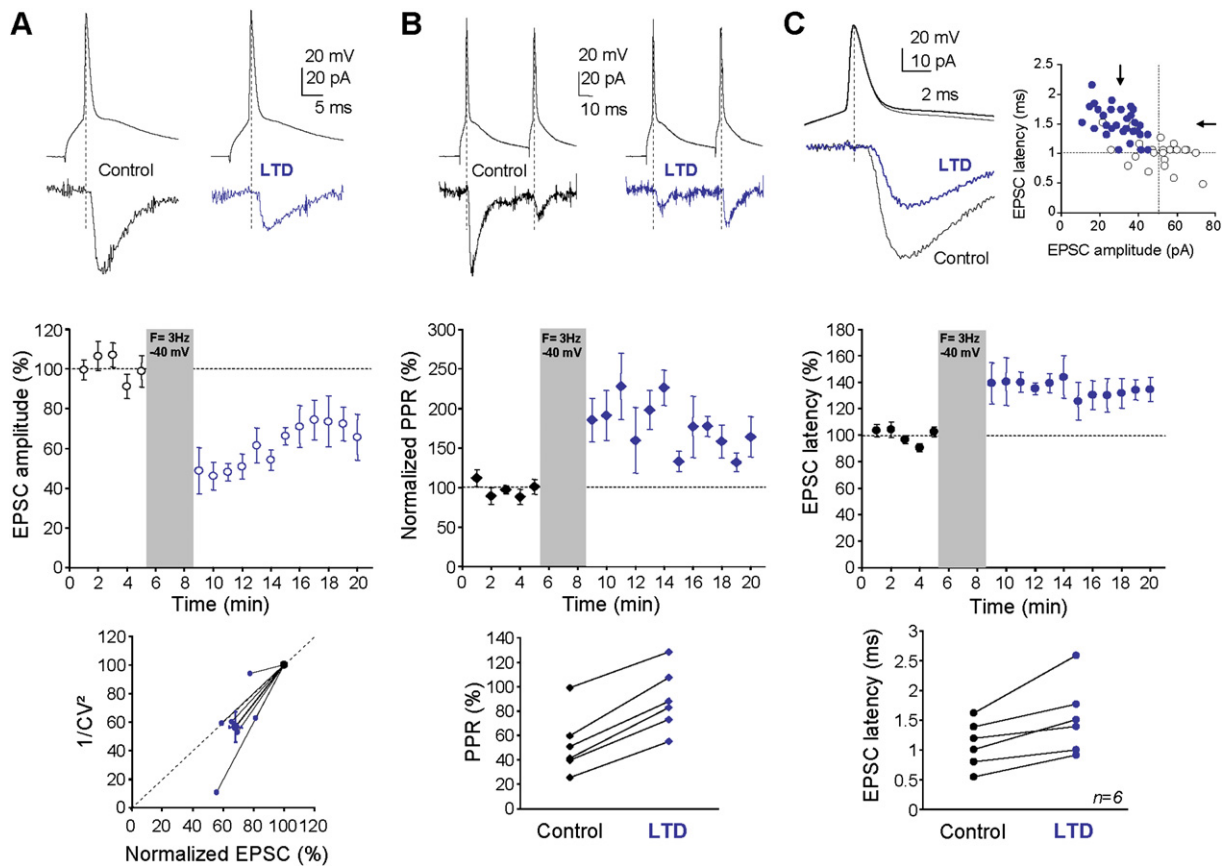
Figure 5. Change in Latency Associated with Presynaptic LTD at L5-L5 Synapse

(A) Presynaptic LTD was induced at L5-L5 connections by repetitively stimulating the presynaptic neuron at 3 Hz while the postsynaptic neuron was held at −40 mV. (Upper traces) Synaptic currents before (control) and after 3 Hz stimulation (LTD). (Middle graph) Normalized time course of the EPSC amplitude. (Lower graph) Normalized $1/CV^2$ versus normalized EPSC amplitude in six experiments (○, individual connections; ●, pooled data).

(B) Enhanced PPR after LTD induction. (Top) Synaptic currents evoked by a pair of presynaptic APs before (control) and 10 min after the low-frequency stimulation (LTD). Note the switch from PPD to PPF. (Middle) Time course of the normalized PPR. (Bottom) Summary of six experiments.

(C) Increased synaptic latency associated with LTD. (Top right) EPSC latency versus EPSC amplitude data in control (○) and after LTD induction (●). (Top left) Representative traces (averaged over 18 trials). (Middle graph) Time course of the normalized changes in EPSC latency. (Bottom) Summary of six experiments.

Error bars show SEM.

Tsodyks, 1996; Sjöström et al., 2003) and/or in the coefficient of variation of EPSC amplitudes (Sjöström et al., 2003), indicating that it may result from a presynaptic change in glutamate release (but see Poncer and Malinow, 2001). We tested whether changes in synaptic latency were observed following induction of a presynaptic form of long-term synaptic plasticity. At L5 pyramidal cell synapses, Pr is high in control conditions (low PPR and little effect of elevation of the $[Ca^{2+}]/[Mg^{2+}]$ ratio). Thus, long-term downregulation of presynaptic efficacy is expected to be easily induced at this synapse. In fact, LTD was reliably induced by stimulating the presynaptic cell at 3 Hz for 3–5 min while the postsynaptic cell was held at −40/−30 mV. After induction, synaptic efficacy was reduced to 63% ± 7% of the control EPSC amplitude (n = 6, Figure 5A), the coefficient of variation was significantly reduced (normalized $1/CV^2 = 57\% \pm 11\%$, n = 6, Figure 5B),

and the PPR was increased (from 53% ± 10% to 89% ± 10%, n = 6, paired t test p < 0.01, Figure 5B), suggesting that presynaptic release was decreased following induction of LTD. Most interestingly, induction of LTD resulted in a long-lasting enhancement of mean latency (141% ± 8%; Figure 5C). In fact, after LTD induction, the latency was found to be increased (from 1.09 ± 0.16 to 1.52 ± 0.24 ms, n = 6; paired t test, p < 0.01). We then induced long-term potentiation (LTP) by stimulating the presynaptic cell at 1 Hz for 2–3 min while the postsynaptic cell was held at −10 mV. After induction, synaptic efficacy (142% ± 7%, n = 4, Figure 6A) and the coefficient of variation ($1/CV^2 = 256\% \pm 12\%$, n = 4) were enhanced, and PPR was decreased (from 73% ± 10% to 42% ± 4%; paired t test, p < 0.01), suggesting a presynaptic facilitation of glutamate release underlying LTP (Figure 6B). Here again, the latency was found to decrease (from
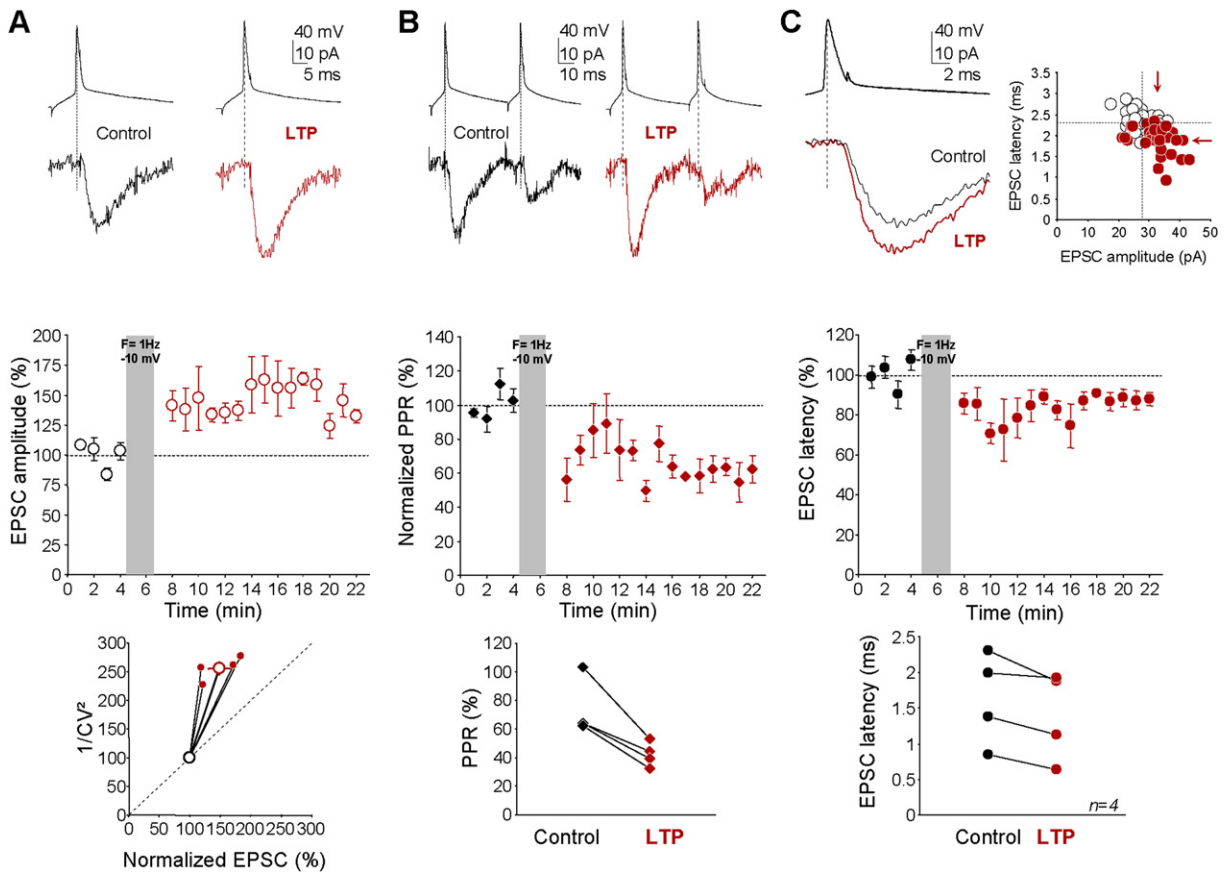
Figure 6. Change in Latency Associated with Presynaptic LTP at L5-L5 Synapse

(A) Presynaptic LTP was induced at L5-L5 connections by repetitively stimulating the presynaptic neuron at 1 Hz while the postsynaptic neuron was held at −10 mV. (Top) Synaptic currents before (control) and after 1 Hz stimulation (LTP). (Middle) Time course of the normalized EPSC amplitude. (Bottom) Normalized $1/CV^2$ versus normalized EPSC amplitude in four experiments (•, individual connections; ○, pooled data).

(B) Decreased PPR after LTP induction. (Upper traces) Synaptic currents evoked by a pair of presynaptic APs before (control) and 10 min after the high-frequency stimulation (LTP). Note the enhancement of PPD. (Middle graph) Time course of the normalized PPR. (Bottom) Summary of four experiments.

(C) Reduction of synaptic latency associated with LTP. (Top) EPSC latency versus EPSC amplitude data in control (○) and after LTP induction (•). (Left) Representative traces (averages over six trials). (Middle graph) Time course of the normalized EPSC latency. (Bottom) Summary of four experiments.

Error bars show SEM.

1.63 ± 0.32 ms to 1.38 ± 0.31 ms, n = 4, paired t test, p < 0.03, Figure 6C). Thus, synaptic latency is also subject to long-term regulation when presynaptic long-term synaptic plasticity is induced.

Incidence of Amplitude-Dependent Variation in Latency on the Input-Output Function

Next, we determined whether amplitude-dependent variation in latency observed following LTD may affect the input-output function of L5 pyramidal neurons. To test this hypothesis, in vivo-like background synaptic conductance was injected using the dynamic-clamp technique (Galarreta and Hestrin, 2001; Zsiros and Hestrin, 2005), and the effect of amplitude-dependent latency variation on EPSP-spike coupling was investigated (Figure 7A). Unitary

synaptic events were triggered in the middle of the background train (at a latency of ∼500 ms). Two conductance amplitudes were used (3.4 nS [250 pA at −70 mV] and 2.2 nS [170 pA at −70 mV]), with two different latencies (respectively, 0 ms and 0.5 ms, see Figure 1C). Importantly, the raster plot and cumulative probability curve were shifted toward long latencies when synaptic conductance was reduced from 3.4 to 2.2 nS with a latency shift of 0.5 ms (n = 16 neurons, Figure 7B). The cumulative probability curve was shifted by 1.1 ms (Mann-Whitney U test, p < 0.005), showing that the amplitude-dependent variation in latency has a significant effect on the activity of the postsynaptic neuron. When a latency shift of 0.5 ms was introduced without changing synaptic conductance, the output message was also shifted by 0.5 ms (n = 16;
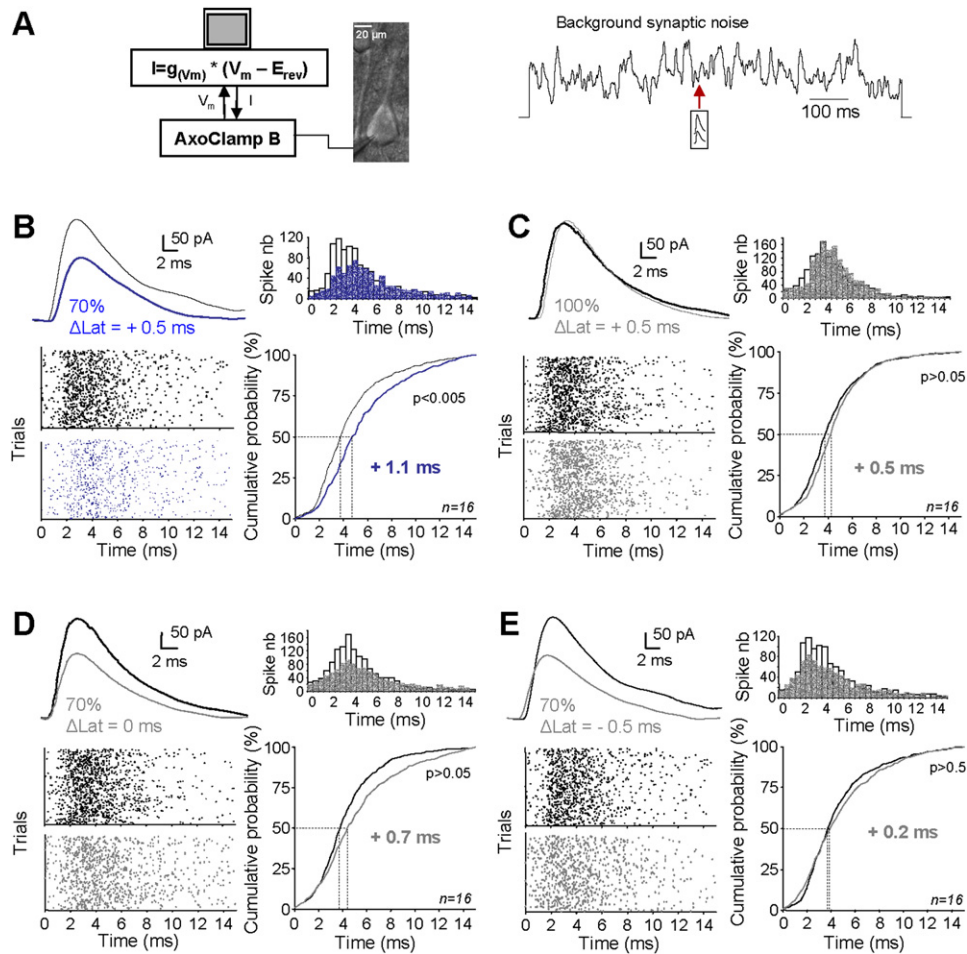
Figure 7. Effect of EPSP Modifications on Input/Output Function in L5 Pyramidal Neurons

(A) (Left) Experimental set-up used for injecting artificial synaptic conductances. An L5 pyramidal neuron was recorded in whole-cell configuration. The dynamic current (I) injected through the recorded electrode was a function of the voltage (V_m) measured continuously. (Right) Injected synaptic signals: combination of background synaptic noise (top trace) and a test or control synaptic conductance.

(B-E) Effects of latency/amplitude variation on output firing. The two parameters amplitude and latency were modified, thus giving four main cases (B–E). EPSC amplitude was set to 100% or 70% of the control, whereas ΔLat was set to 0.5, 0 ms, or −0.5 ms. Each raster plot, histogram, or cumulative probability curve is the pool of 16 experiments (3200 trials [200 trials/neuron]). Input (top left) and output signals (bottom left, raster plots) for each type of synaptic conductance. (B) Effect of reducing EPSC amplitude (70% of the control) and increasing synaptic latency (ΔLat = + 0.5 ms) (i.e., mimicking presynaptic LTD). (C) Effect of modifications in synaptic latency (ΔLat = + 0.5 ms) with a fixed EPSC amplitude (here 250 pA). (Top left) Input signals in control (black) and with a delay of 0.5 ms (gray). The delay of 0.5 ms of the input shifted the spiking histogram and the cumulative probability curves for spiking activity by the same value (0.5 ms). (D) Effect of reducing EPSP amplitude without changing synaptic latency (ΔLat = 0 ms) on input/output function. The 30% reduction of the synaptic current (from 250 to 170 pA) delayed postsynaptic firing by 0.7 ms (see PSTHs and cumulative probability curves). (E) Effect of reducing EPSP amplitude (70% of the control) and decreasing synaptic latency (ΔLat = −0.5 ms). The two changes opposed each other, and no significant modification of postsynaptic firing was observed.

Figure 7C). Interestingly, reduction of synaptic conductance without any change in the latency, delayed the output firing by 0.7 ms (n = 16; Figure 7D). Finally, the opposite configuration was tested where the reduction in amplitude was associated with a shortening of the latency by 0.5 ms (Figure 7E). In these conditions, the two effects compensate each other, and the net effect on postsynaptic spiking was nearly zero. Thus, our findings show that the inverse amplitude-latency variation represents an optimal configuration to affect the timing of the output message.

DISCUSSION

Release-Dependent Variation in Latency at L5-L5 Synapses

We show here that synaptic latency between pairs of L5 neurons varies within 1–2 ms in an amplitude-dependent manner such that large-amplitude EPSCs had comparatively shorter latencies. The long latency observed for small events could not be attributed to poor detection of small postsynaptic currents because postsynaptic

reduction of EPSC amplitude with NBQX did not affect synaptic latency. In addition, when the signal-to-noise ratio was improved by averaging small EPSCs, the dependence of the latency on the amplitude of EPSCs was still reliably observed. Furthermore, the time course of small and large EPSCs was not significantly different, indicating that the difference in latency observed between small and large EPSCs is unlikely to result from differential dendritic filtering.

Whereas postsynaptic manipulations had no effect, manipulations that modified Pr significantly affected synaptic latency. Presynaptic reduction of synaptic transmission induced by decreasing the $[Ca^{2+}]/[Mg^{2+}]$ ratio or by applying the $GABA_B$ receptor agonist baclofen significantly increased the latency. Conversely, the increment in presynaptic Pr obtained after increasing the $[Ca^{2+}]/[Mg^{2+}]$ ratio reduced synaptic latency. Thus, the amplitude-dependent variation in latency demonstrated here is of presynaptic origin and is largely determined by changes in Pr.

Variation in synaptic latency has also been observed at the crustacean neuromuscular junction. Phasic synapses display a high Pr, whereas tonic synapses are nearly unresponsive to single APs. It is important to note that these synapses are associated, respectively, with short and long synaptic delay (Millar et al., 2005). Our observation agrees with this study but also extends our understanding of this phenomenon by showing that, depending on Pr, the same L5-L5 connection or CA3-CA3 connection displays short or long latencies.

Possible Mechanisms of Pr-Dependent Latency

What is the mechanism underlying amplitude-dependent variation in latency? First, a combination of axonal geometry with a heterogeneous Pr at specific release sites may account for the release-dependent latency. This hypothesis is supported by the fact that, at L5-L5 contacts, the presynaptic axon establishes four to eight synaptic contacts with an individual L5 pyramidal neuron on different dendritic sites (Markram et al., 1997). Although the number of putative contacts was not determined here by a morphological analysis, mean-variance analysis of the EPSC fluctuations in different release conditions (control, $[Mg^{2+}]/[Ca^{2+}]$ ratio = 0.33 or $[Mg^{2+}]/[Ca^{2+}]$ ratio = 0.1) suggests the presence of approximately ten release sites (S.B. and D.D., unpublished data). Thus, manipulating presynaptic Pr could specifically affect synapses located at different distances along the axons/axon collaterals. Although this possibility cannot be ruled out, it appears unlikely because this scheme would require a defined geometrical configuration of boutons with high Pr. In fact, according to this hypothesis, high Pr boutons should be located at distal axonal sites, which has never been reported at cortical axons. Furthermore, the selective sampling of short latencies within a population of heterogeneous latency is unlikely because very short latencies were never encountered under conditions of low Pr. Moreover, in contrast with our observations, this hypothesis predicts that the time-to-peak would be longer for large EPSCs. In addition,

amplitude-dependent latency variations have been observed in the cerebellum at single-site GABAergic synapses (Auger et al., 1998). Thus, alternative mechanisms involving the release machinery must be considered.

We show here that manipulations of the external $[Ca^{2+}]/[Mg^{2+}]$ ratio or application of baclofen affected synaptic latency. The reduction of the $[Ca^{2+}]/[Mg^{2+}]$ ratio or the application of baclofen reduces the intracellular $[Ca^{2+}]$. Our data are consistent with the Ca^{2+}-dependent variation in synaptic delay observed at the calyx of Held synapse (Bollmann et al., 2000; Schneggenburger and Neher, 2000; Felmy et al., 2003; Bollmann and Sakmann, 2005; Feldchyshyn and Wang, 2007) or at the neuromuscular junction (Millar et al., 2005). These studies have led to a consensus model assuming that five Ca^{2+} ions bind the Ca^{2+} sensor in a cooperative fashion before vesicle fusion occurs at a constant rate. Thus, intraterminal $[Ca^{2+}]$ would directly underlie the variation in synaptic delay. Small increases in presynaptic $[Ca^{2+}]$ result in vesicular release with a long delay because cooperativity among Ca^{2+} ions is a limiting factor. This finding explains at least in part the excellent fit by a logarithmic function of the latency-amplitude relationship, in agreement with variations in synaptic delay induced by photolysis of presynaptic caged Ca^{2+} at the calyx of Held (Bollmann et al., 2000; Schneggenburger and Neher, 2000) or at the neuromuscular junction (Millar et al., 2005).

In conclusion, two main mechanisms are proposed to account for release-dependent latencies: 1) the cooperative nature of the release process and/or 2) heterogeneity in the distance between Ca^{2+} sensors controlling releasable vesicles and Ca^{2+} channels (Neher, 1998).

Short-Term Plasticity and Synaptic Latency

Synaptic latency was also observed to change when presynaptic glutamate release was altered following induction of short- and long-term plasticity. In agreement with the depletion model, short-term facilitation and depression occurred from trial to trial, and the amplitudes of the first and the second EPSPs were found to be inversely correlated (Debanne et al., 1996). As a consequence, paired-pulse depression and facilitation were associated, respectively, with increased and decreased synaptic latencies. In fact, the variation in latency was cumulative during short-term plasticity, and the total range was largely above 1 ms. Furthermore, changes in paired-pulse ratio induced by manipulation of the $[Mg^{2+}]/[Ca^{2+}]$ ratio determined the variations in latency in a predictable manner. Taken together, these data strongly support the fact that short-term dynamics of synaptic strength modulate the timing of synaptic responses.

Increased synaptic latency associated with PPD has been reported at the Mauthner axon-interneuron synapse of the goldfish (Waldeck et al., 2000), whereas reduced synaptic latency occurring with PPF is observed at the neuromuscular junction of the crayfish (Vyshedskiy et al., 2000). We show here that the second AP was broadened at the somatic level when paired-pulse stimulation was

tested with an interval of 50 ms, but the spike waveform was virtually unchanged in axons at a distance larger than 50 μm from the soma. APs in the presynaptic terminal may, however, be broadened during repetitive stimulation (Geiger and Jonas, 2000). Since this prolongation was estimated to be smaller than 3% for two spikes at 50 Hz at mossy fiber boutons (Geiger and Jonas, 2000), it is unlikely to have affected our results. In addition, presynaptic spike broadening could not account for the negative variation in synaptic latency observed with paired-pulse facilitation. Thus, variations in latency observed during short-term plasticity are unlikely to result from modifications of the presynaptic AP waveform but rather are related to a mechanism implicating the presynaptic release machinery and/or events that occur downstream of Ca^{2+} influx.

Long-Term Plasticity and Synaptic Latency
Variations in synaptic latency are not limited to short-term synaptic plasticity but can also be observed following induction of long-lasting synaptic plasticity. LTD induced at L5-L5 synapses reduced synaptic strength, an effect that was associated with a marked increase in paired-pulse ratio and a decrease in the CV^{-2}, pointing to a mainly presynaptic expression site of neocortical LTD (Sjöström et al., 2003). Importantly, as expected from the observation of release-dependent latency for individual synaptic events, synaptic latency was prolonged by 40% following induction of LTD. Like the reductions in Pr produced by decreasing the extracellular $[Ca^{2+}]/[Mg^{2+}]$ ratio or by applying baclofen, LTD induction shifted the data points toward longer latencies along the inverse correlation axis (Figure 5C). Conversely, induction of a presynaptic form of LTP decreased the latency at monosynaptic contacts. Thus, our data indicate that regulation of Pr is consistently associated with a change in synaptic latency, suggesting that the latency shift could be considered as a major physiological hallmark of presynaptic changes in transmission.

Furthermore, our results suggest a general rule for latency variations in synaptic circuits because the inverse correlation observed for short- and long-term plasticity (Figure 8) seems to be also valid for the latency of polysynaptic responses. As APs evoked by monosynaptic EPSPs in interposed neurons were shown to be shorter after induction of short-term facilitation or LTP and delayed after induction of short-term depression and LTD (Andersen et al., 1980; Daoudal et al., 2002), polysynaptic EPSPs may also obey the rule that we have discovered for monosynaptic responses (Komatsu et al., 1998; S.B. and D.D., unpublished data). Thus, reduced latencies in reinforced circuits and delayed responses in nonreinforced circuits appear to be a general feature of short- and long-term cortical plasticity.

Functional Relevance of Amplitude-Dependent Variations in Latency
Amplitude variations originating from presynaptic short- or long-term plasticity determine the timing of synaptic transmission in the millisecond range. How do these vari-
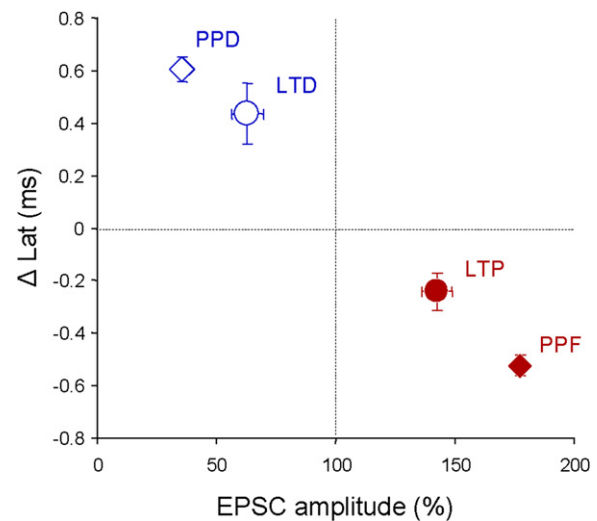

Figure 8. Activity-Dependent Changes in Latency at L5-L5 Connection

Latency variations (ΔLat) are expressed as a function of EPSC amplitude following short- and long-term synaptic plasticity. Synaptic facilitation (PPF and LTP) shortens synaptic latency, whereas synaptic depression (PPD and LTD) prolongs latency. Error bars show SEM.

ations affect postsynaptic spiking activity? The postsynaptic impact of a change in latency only can be easily predicted: a small shift in latency at the input side produces an equivalent shift at the output side. The effect of a concomitant change in latency is more complex. When a reduction in amplitude and an increase in latency, as seen following LTD induction, were mimicked using the dynamic-clamp, the two effects were additive, and the postsynaptic discharge evoked by the simulated EPSP was significantly shifted toward longer latencies. Consistent with previous observations (Fetz and Gustafsson, 1983; Xu-Friedman and Regehr, 2005), the histogram of output firing was broader and shifted toward longer latencies when the EPSC amplitude was reduced by 30% at the input side. Interestingly, the reverse combination produced no significant change in postsynaptic firing. Thus, the amplitude-dependent change in synaptic delay we report here appears to be a favorable combination to efficiently affect the input-output timing at cortical synapses. In physiological conditions, a presynaptic AP can be elicited by the stimulation of a compound synaptic pathway. The temporal jitter of the presynaptic spike was 0.58 ms, as previously observed in the hippocampus (Pouille and Scanziani, 2001). This value was found to be clearly insufficient to blur the significant correlation between EPSC latency and EPSC amplitude. Thus, our data indicate that Pr-dependent latency can be observed in cortical networks activated by synaptic stimulation.

What is the functional significance of variations in synaptic latency for network behavior? Theoretical work shows that both synchronization of cortical columns and network resonance depend on latency (Bush and Sejnowski, 1996;

Maex and De Schutter, 2003). A recent theoretical study emphasizes the importance of this delay in the emergence of polysynchronization in neural networks (Izhikevitch, 2006). In most computational studies of storage capacity, synaptic delay is totally ignored, but the interplay between latencies and synaptic plasticity based on timing (spike-timing-dependent plasticity [STDP]) in fact generates polychronous groups (i.e., strongly interconnected groups of neurons that fire with millisecond precision). Most importantly, the number of groups of neurons that can fire synchronously exceeds the number of neurons in a network, resulting in a system with massive memory capacity (Izhikevitch, 2006). Thus, it will be particularly interesting to evaluate whether release-dependent variations in synaptic latency further increase storage capacity.

A Novel Code for Synaptic Dynamics?

Short- or long-term synaptic plasticity is considered to be the main mechanism allowing activity- and time-dependent changes in network function during adaptive processes. Neuronal timing is usually converted into variations in synaptic strength. For instance, depressing synapses transform time intervals into voltage amplitudes (Grande and Spain, 2005). Here we show that in addition to these classical schemes, variations in synaptic strength occurring during physiological activity patterns are also converted into variations in time according to a simple rule. These variations have a significant impact on postsynaptic firing, and its incidence on the timing of realistic neuronal networks must now be determined. Although this question is still pending, one may propose that this simple rule may unite the "*rate code*" where information is encoded by the strength of the neuronal responses (Barlow, 1972) and the "*time code*" based on the relative timing of neuronal events (Singer, 1999).

EXPERIMENTAL PROCEDURES

Slices and Slice Cultures
Cortical slices (350–400 μm thick) were obtained from 13- to 20-day-old Wistar rats as previously described (Carlier et al., 2006). All experiments were carried out according to the European and Institutional guidelines for the care and use of laboratory animals (Council Directive 86/609/EEC and French National Research Council). Rats were deeply anesthetized with chloral hydrate (intraperitoneal, 200 mg kg-1) and killed by decapitation. Slices were cut in an ice-cold solution containing (in mM) 280 sucrose, 26 NaHCO₃, 10 D-glucose, 10 MgCl₂, 1.3 KCl, and 1 CaCl₂ and were bubbled with 95% O₂/5% CO₂, pH 7.4. Slices recovered (1 hr) in a solution containing (in mM) 125 NaCl, 26 NaHCO₃, 3 CaCl₂, 2.5 KCl, 2 MgCl₂, 0.8 NaH₂PO₄, and 10 D-glucose and were equilibrated with 95% O₂/5% CO₂.

Interface hippocampal slice cultures were prepared as described previously (Stoppini et al., 1991). In brief, hippocampal slices (250 μm) were obtained from 6- to 10-day-old Wistar rats and were grown on culture inserts. Culture medium was replaced three times per week. Slice cultures were maintained at 35°C for at least 4–5 days in vitro before experiments.

Each slice or slice culture was transferred to a submerged chamber mounted on an upright microscope (Olympus). L5 pyramidal neurons were visualized using DIC infrared videomicroscopy. The identity of the recorded neurons was confirmed by their firing pattern in response to depolarizing pulses of current and occasionally by their morphology revealed with biocytin labeling (Figure 1A). Briefly, biocytin (0.3%, Sigma) was added to the pipette solution and was revealed with avidin-biotin complex coupled to fluorescein.

Recording and Data Analysis
Dual whole-cell recordings were made at 34°C in a temperature-controlled recording chamber (Luigs and Neumann, Ratingen, Germany). The external solution contained (in mM) 125 NaCl, 26 NaHCO₃, 3 CaCl₂, 2.5 KCl, 2 MgCl₂, 0.8 NaH₂PO₄, and 10 D-glucose and was equilibrated with 95% O₂/5% CO₂. Patch pipettes (5–10 MΩ) were filled with a solution containing (in mM) 120 K-gluconate, 20 KCl, 10 HEPES, 0.5 EGTA, 2 Na₂ATP, 0.3 NaGTP, and 2 MgCl₂, pH 7.4. Some experiments were performed with another postsynaptic pipette solution containing (in mM) 140 CsMeSO₄, 10 HEPES, 5 EGTA, 4 MgATP, and 0.3 NaATP, pH 7.3. Classically, the presynaptic neuron was recorded in current-clamp with an Axoclamp 2B amplifier (Axon Instruments) and the postsynaptic cell in voltage-clamp with an Axopatch 200B amplifier (Axon Instruments). Pre- and postsynaptic cells were held at their resting membrane potential (−65/−70 mV). Presynaptic APs were generated by injecting brief pulses (5–10 ms) depolarizing pulses of current at a frequency of 0.1 Hz. The voltage and current signals were low-pass filtered (3 kHz), and acquisition of 500 ms sequences was performed at 10–15 kHz with the software Acquis1 (G. Sadoc, CNRS Gif-sur-Yvette France) or DAAD (N. Ankri, INSERM UMR 641 Marseille France).

Synaptic responses could be averaged following alignment of the presynaptic APs using automatic peak detection (Detectivent, N. Ankri INSERM; Figure S1A). The presence or absence of a synaptic connection between two neurons was determined on the basis of averages of 30 to 50 individual traces, including failures. With this technique even very small responses (<0.2 mV or <10 pA) could be easily detected. In practice, the smaller averaged synaptic responses were 0.1 mV and 4 pA, as previously observed (Debanne et al., 1995).

High-frequency components in the signals were filtered with a median filter (rank 1 or 2), and in some cases a de-noising filtering (wavelet methods) was used. Special care was taken to verify that filtering of signals did not affect the original signals by superposition of the raw and filtered signals (Figure S1B).

Latency of EPSC onset was defined as the time from the peak of the AP to 5% of the EPSC amplitude (Markram et al., 1997; Figure S1C). EPSC amplitudes were measured by averaging 20 to 60 trials according to their respective amplitudes.

Role of the Presynaptic Jitter
To determine the effect of presynaptic spike jitter, the latency distribution was convolved with a Gaussian function with a standard deviation of σ = 0.58 ms (previously determined as shown in Figure 2A). In fact, for each latency value, a random value was added. Each random value was drawn according to a normal rule with a standard deviation (σ = 0.58 ms) and a mean equal to 0.

In a second step, the coefficient of linear correlation in the resulting amplitude-latency distribution was calculated, and the Student's t test was applied to evaluate the significance with two criteria (p < 0.05 or p < 0.005). These two operations were iterated 10⁵ times, and the rate of success was calculated (Figure 2D).

Induction Protocols for Short- and Long-Term Synaptic Plasticity
Short-term synaptic plasticity was tested by eliciting pairs of presynaptic APs with short depolarizing current pulses (10–20 ms, 0.2–0.7 nA) separated by 50 ms. Pairs of pulses were delivered at intervals of 10 s. LTD was induced by a low-frequency stimulation protocol in which the presynaptic cell was stimulated at 3 Hz for 3–5 min, and the postsynaptic neuron was held at a membrane potential of −40 mV. LTP was induced by stimulating the presynaptic cell at 1 Hz during 2–3 min while the postsynaptic cell was held at −10 mV.

Simulation of Background Postsynaptic Conductance

To simulate the background synaptic conductance, we constructed waveforms by combining excitatory and inhibitory conductance waveforms (Galaretta and Hestrin, 2001; Zsiros and Hestrin, 2005). The unitary excitatory and inhibitory postsynaptic conductance transients were estimated using excitatory and inhibitory synaptic currents (EPSCs and IPSCs) previously obtained in paired recordings or in minimal stimulations. The profile of EPSCs and IPSCs was determined by two exponentials (EPSC-rise time [10%–90%] = 2.7 ms [τ_{on} = 1.6 ms] and τ_{decay} = 7 ms, IPSC-rise time = 1.8 ms [τ_{on} = 1.3 ms] and τ_{decay} = 7 ms). The conductance transients were convolved with Poisson trains at 1000 Hz to generate the excitatory and 500 Hz to generate the inhibitory conductance waveforms. The amplitudes of the excitatory and inhibitory unitary conductances were 0.3 and 0.2 nS. The burst of AMPA-like (E_{rev} = 0 mV) EPSPs and GABA$_A$-like (E_{rev} = −70 mV) IPSPs was simulated by a dynamic-clamp amplifier (SM1; Cambridge Conductance, Cambridge, UK) fed by a digital-analog converter (UEIdaq board) and driven by DAAD software. The resulting background noise elicited ~12 to 22 spikes on each 950 ms trial.

To test the incidence of amplitude-dependent variation in latency, a single synaptic event was generated in the middle of the background noise (latency of 462 ms). The time course of the synaptic conductance was as described above, and the main characteristics of the synaptic currents (amplitude and latency) were taken from the data illustrated in Figure 1C. The amplitude and latency varied in a discrete manner, and two amplitudes were considered here. Synaptic conductances smaller than 0.5 nS were found to produce no clear modulation in the firing activity. Therefore, the conductance of the large event was 3.42 nS with a latency of 0 ms, whereas the conductance of the small event was 2.13 nS with a latency of 0.5 ms.

Drugs and Statistical Analysis

NBQX [6-nitro-7-sulphamoylbenzo(*f*)quinoxaline-2,3-dione] was purchased from Tocris Cookson. Baclofen was obtained from Sigma. Data are presented as means ± SEM.

Supplemental Data

The Supplemental Data for this article can be found online at http://www.neuron.org/cgi/content/full/56/6/1048/DC1/.

REFERENCES

Andersen, P., Sundberg, S.H., Sveen, O., Swann, S.W., and Wigström, H. (1980). Possible mechanisms for long-lasting potentiation of synaptic transmission in hippocampal slices from guinea pigs. J. Physiol. *302*, 463–482.

Auger, C., Kondo, S., and Marty, A. (1998). Multivesicular release at single functional synaptic sites in cerebellar stellate and basket cells. J. Neurosci. *18*, 4532–4557.

Augustine, G.J., Charlton, M.P., and Smith, S.J. (1985). Calcium entry and transmitter release at voltage-clamped nerve terminals of squid. J. Physiol. *369*, 163–181.

Barlow, H.B. (1972). Single units and cognition: a neurone doctrine for perceptual psychology. Perception *1*, 371–394.

Bi, G.Q., and Poo, M.M. (1998). Synaptic modifications in cultured hippocampal neurons: dependence on spike-timing, synaptic strength, and postsynaptic cell type. J. Neurosci. *18*, 10464–10472.

Bollmann, J.H., and Sakmann, B. (2005). Control of synaptic strength and timing by the release-site Ca^{2+} signal. Nat. Neurosci. *8*, 426–434.

Bollmann, J.H., Sakmann, B., and Borst, J.G.G. (2000). Calcium sensitivity of glutamate release in a Calyx-type terminal. Science *289*, 953–957.

Bush, P., and Sejnowski, T.J. (1996). Inhibition synchronizes connected cortical neurons within and between columns in realistic networks models. J. Comput. Neurosci. *3*, 91–110.

Carlier, E., Sourdet, V., Boudkkazi, S., Deglise, P., Ankri, N., Fronzaroli-Molinieres, L., and Debanne, D. (2006). Metabotropic glutamate receptor subtype 1 regulates sodium currents in rat neocortical pyramidal neurons. J. Physiol. *577*, 141–154.

Daoudal, G., Hanada, Y., and Debanne, D. (2002). Bidirectional plasticity of excitatory postsynaptic potential (EPSP)-spike coupling in CA1 hippocampal pyramidal neurons. Proc. Natl. Acad. Sci. USA *99*, 14512–14517.

Debanne, D. (2004). Information processing in the axon. Nat. Rev. Neurosci. *5*, 304–316.

Debanne, D., Guérineau, N.C., Gähwiler, B.H., and Thompson, S.M. (1995). Physiology and pharmacology of unitary synaptic connections between pairs of cells in areas CA3 and CA1 of rat hippocampal slice cultures. J. Neurophysiol. *73*, 1282–1294.

Debanne, D., Guérineau, N.C., Gähwiler, B.H., and Thompson, S.M. (1996). Paired-pulse facilitation and depression at unitary synapses in rat hippocampus: quantal fluctuation affects subsequent release. J. Physiol. *491*, 163–176.

Debanne, D., Gähwiler, B.H., and Thompson, S.M. (1998). Long-term synaptic plasticity between pairs of individual CA3 pyramidal neurons. J. Physiol. *507*, 237–247.

Feldchyshyn, M.J., and Wang, L.Y. (2007). Activity-dependent changes in temporal components of neurotransmission at the juvenile mouse calyx of Held synapse. J. Physiol. *581*, 581–602.

Feldmeyer, D., Egger, V., Lübke, J., and Sakmann, B. (1999). Synaptic connections between spiny layer 4 neurones in the "barrel field" of rat somatosensory cortex. J. Physiol. *521*, 169–190.

Felmy, F., Neher, E., and Schneggenburger, R. (2003). Probing the intracellular calcium sensitivity of transmitter release during synaptic facilitation. Neuron *37*, 801–811.

Fetz, E.E., and Gustafsson, B. (1983). Relation between shapes of post-synaptic potentials and changes in firing probability of cat motoneurones. J. Physiol. *341*, 387–410.

Fricker, D., and Miles, R. (2000). EPSP amplification and the precision of spike timing in hippocampal neurons. Neuron *28*, 559–569.

Gähwiler, B.H. (1981). Organotypic monolayer cultures of nervous tissue. J. Neurosci. Methods *4*, 329–342.

Galaretta, M., and Hestrin, S. (2001). Spike transmission and synchrony detection in networks of GABAergic interneurons. Science *292*, 2295–2299.

Geiger, J.R.P., and Jonas, P. (2000). Dynamic control of presynaptic Ca2+ inflow by fast-inactivating K+ channels in hippocampal mossy fiber boutons. Neuron *28*, 927–939.

Grande, L.A., and Spain, W.J. (2005). Synaptic depression as a timing device. Physiology (Bethesda) 20, 201–210.

Izhikevitch, E.M. (2006). Polychronization: computation with spikes. Neural Comput. 18, 245–282.

Katz, B., and Miledi, R. (1967). A study of synaptic transmission in the absence of nerve impulses. J. Physiol. 192, 407–436.

Komatsu, Y., Fujii, K., Maeda, J., Sakoguchi, H., and Toyama, K. (1998). Long-term potentiation of synaptic transmission in kitten visual cortex. J. Neurophysiol. 59, 124–141.

König, P., Engel, A.K., and Singer, W. (1996). Integrator or coincidence detector? The role of the cortical neuron revisied. Trends Neurosci. 19, 130–137.

Lin, J.W., and Faber, D.S. (2002). Modulation of synaptic delay during synaptic plasticity. Trends Neurosci. 25, 449–455.

Maex, R., and De Schutter, E. (2003). Resonant synchronization in heterogeneous networks of inhibitory neurons. J. Neurosci. 23, 10503–10514.

Markram, H., and Tsodyks, M. (1996). Redistribution of synaptic efficacy between neocortical pyramidal neurons. Nature 382, 807–810.

Markram, H., Lübke, J., Frotscher, M., Roth, A., and Sakmann, B. (1997). Physiology and anatomy of synaptic connections between thick tufted pyramidal neurones in the developing rat neocortex. J. Physiol. 500, 409–440.

Meinrenken, C.J., Borst, J.G.G., and Sakmann, B. (2003). Local routes revisited: the space and time dependence of the Ca2+ signal for transmitter release at the rat calyx of Held. J. Physiol. 547, 665–689.

Miles, R., and Wong, R.K.S. (1986). Excitatory synaptic interactions between CA3 neurones in the guinea-pig hippocampus. J. Physiol. 373, 397–418.

Millar, A.G., Zucker, R.S., Ellis-Davis, G.C.R., Charlton, M.P., and Atwood, H.L. (2005). Calcium sensitivity of neurotransmitter release differs at phasic and tonic synapses. J. Neurosci. 25, 3113–3125.

Neher, E. (1998). Vesicle pools and Ca2+ microdomains: new tools for understanding their roles in neurotransmitter release. Neuron 20, 389–399.

Poncer, J.C., and Malinow, R. (2001). Postsynaptic conversion of silent synapses during LTP affects synaptic gain and transmission dynamics. Nat. Neurosci. 4, 989–996.

Pouille, F., and Scanziani, M. (2001). Enforcement of temporal fidelity in pyramidal cells by somatic feed-forward inhibition. Science 293, 1159–1163.

Reyes, A., and Sakmann, B. (1999). Developmental switch in the short-term modification of unitary EPSPs evoked in layer 2/3 and layer 5 pyramidal neurons of rat neocortex. J. Neurosci. 19, 3827–3835.

Rieke, F., Warland, D., de Ruyter van Steveninck, R., and Bialek, W. (1997). Spikes: Exploring the Neural Code (Cambridge, MA: MIT Press).

Sabatini, B.L., and Regher, W.G. (1999). Timing of synaptic transmission. Annu. Rev. Physiol. 61, 521–542.

Schneggenburger, R., and Neher, E. (2000). Intracellular calcium dependence of transmitter release rates at a fast central synapse. Nature 406, 889–893.

Singer, W. (1999). Neuronal synchrony: a versatile code for the definition of relations? Neuron 24, 49–65.

Sjöström, P.J., Turrigiano, G.G., and Nelson, S.B. (2003). Neocortical LTD via coincident activation of presynaptic NMDA and cannabinoid receptors. Neuron 39, 641–654.

Sourdet, V., Russier, M., Daoudal, G., Ankri, N., and Debanne, D. (2003). Long-term enhancement of neuronal excitability and temporal fidelity mediated by metabotropic glutamate receptor subtype 5. J. Neurosci. 23, 10238–10248.

Stoppini, L., Buchs, P.A., and Müller, D. (1991). A simple method for organotypic cultures of nervous tissue. J. Neurosci. Methods 37, 173–182.

Thomson, A.M., Deuchars, J., and West, D.C. (1993). Large, deep layer pyramid-pyramid single axon EPSPs in slices of rat motor cortex display paired pulse and frequency-dependent depression, mediated presynaptically and self-facilitation, mediated postsynaptically. J. Neurophysiol. 70, 2354–2369.

Vyshedskiy, A., Allana, T., and Lin, J.W. (2000). Analysis of presynaptic Ca2+ influx and transmitter release kinetics during facilitation at the inhibitor of the crayfish neuromuscular junction. J. Neurosci. 20, 6326–6332.

Waldeck, R.F., Pereda, A., and Faber, D.S. (2000). Properties and plasticity of paired-pulse depression at a central synapse. J. Neurosci. 20, 5312–5320.

Xu-Friedman, M.A., and Regehr, W.G. (2005). Dynamic-clamp analysis of the effects of convergence on spike timing. I. Many synaptic inputs. J. Neurophysiol. 94, 2512–2525.

Zsiros, V., and Hestrin, S. (2005). Background synaptic conductance and precision of EPSP-spike coupling at pyramidal cells. J. Neurophysiol. 93, 3248–3256.

Zucker, R.S., and Regher, W.G. (2002). Short-term synaptic plasticity. Annu. Rev. Physiol. 64, 355–405.